



Universiteit
Leiden
The Netherlands

Stroke and migraine: Translational studies into a complex relationship

Mulder, I.A.

Citation

Mulder, I. A. (2020, November 5). *Stroke and migraine: Translational studies into a complex relationship*. Retrieved from <https://hdl.handle.net/1887/138093>

Version: Publisher's Version

License: [Licence agreement concerning inclusion of doctoral thesis in the Institutional Repository of the University of Leiden](#)

Downloaded from: <https://hdl.handle.net/1887/138093>

Note: To cite this publication please use the final published version (if applicable).

Cover Page



Universiteit Leiden

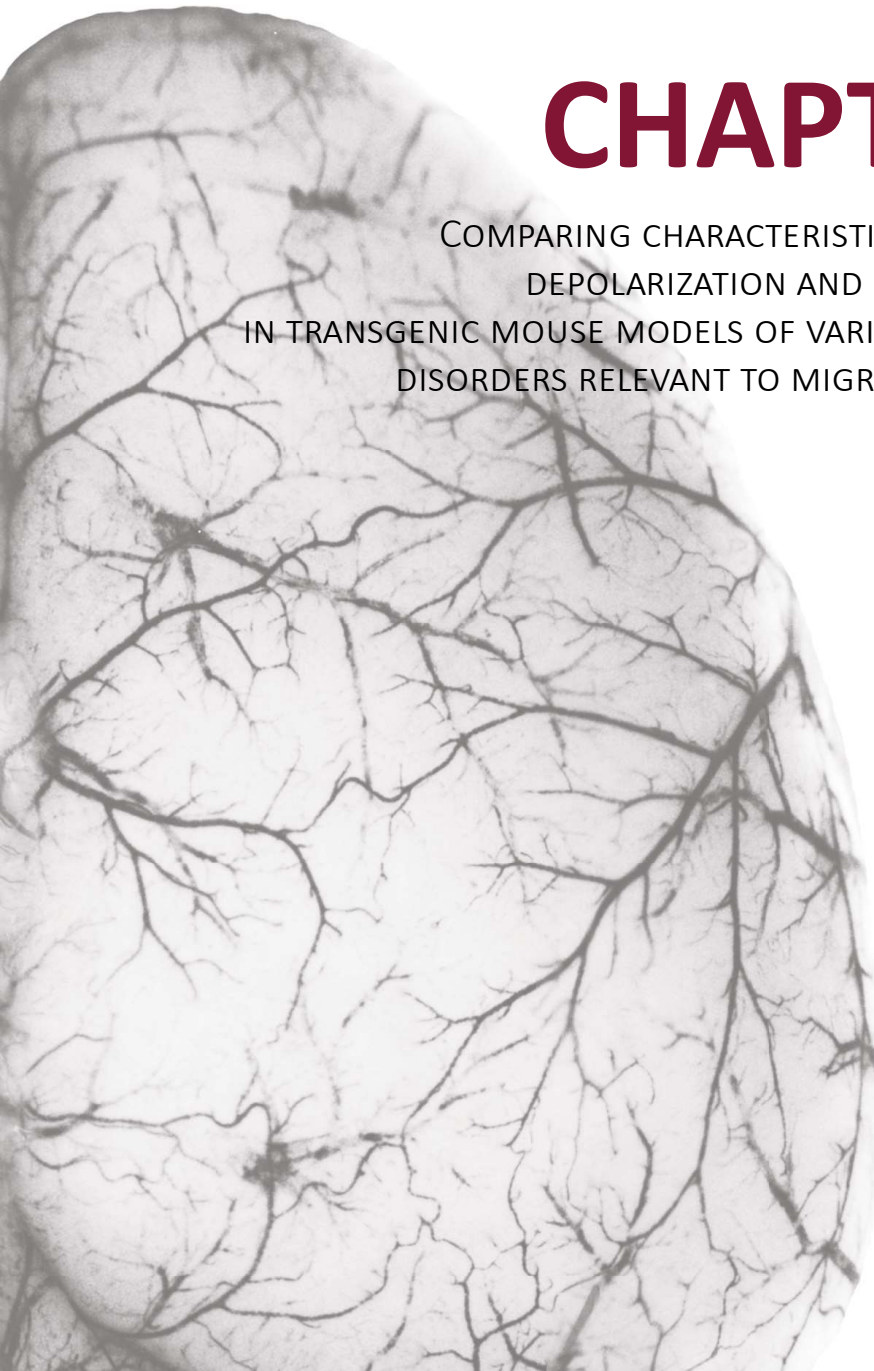


The handle <http://hdl.handle.net/1887/138093> holds various files of this Leiden University dissertation.

Author: Mulder, I.A.

Title: Stroke and migraine: Translational studies into a complex relationship

Issue Date: 2020-11-05



CHAPTER 6

COMPARING CHARACTERISTICS OF SPREADING
DEPOLARIZATION AND ISCHEMIC STROKE
IN TRANSGENIC MOUSE MODELS OF VARIOUS MONOGENIC
DISORDERS RELEVANT TO MIGRAINE AND STROKE

Mulder IA, van Heiningen SH, Broos LAM, Ferrari MD, Tolner EA,
Wermer MJH and van den Maagdenberg AMJM

ABSTRACT

Migraine and stroke have both been linked to monogenetic FHM1, CADASIL and RVCL-S, but it is not understood what mechanisms underlie this relation. Comparing characteristics of migraine and ischemic stroke in transgenic mouse models with pathogenic gene mutations for these diseases can be instrumental to dissect to what extent neuronal (FHM1) and vascular mechanisms (CADASIL, RVCL-S) contribute to disease pathology.

Cortical spreading depolarization (CSD) and transient middle cerebral artery occlusion (MCAO), as experimental surrogates of migraine aura and ischemic stroke, respectively, were induced in young (3- to 6-month-old; both CSD and MCAO) and/or old (12- to 14-month-old; only MCAO) FHM1, CADASIL and RVCL-S mutant mice. As measures of CSD susceptibility, frequency and propagation rate were assessed. Anoxic depolarization latency during MCAO as well as infarct volume and neurologic deficit before and following MCAO were studied to assess susceptibility to stroke. For each strain, mutant mice were compared to the appropriate wild-type controls.

Only young FHM1 mutant mice showed abnormal, increased CSD frequency (18.3 ± 0.6 vs 9.7 ± 0.7 , $p < 0.001$) and propagation rate (5.4 ± 0.7 vs 3.3 ± 0.5 , $p = 0.009$). Anoxic depolarization latency was overall decreased in both the FHM1 ($F(1, 24) = 7.928$, $p = 0.01$) and CADASIL ($F(1, 22) = 16.377$, $p = 0.001$) mutant mice. Infarct volume was increased only in RVCL-S mutant mice ($p = 0.005$ for pooled age groups, but mainly driven by the older mice) and correlated with increased neurologic deficit after infarct ($p = 0.005$).

Both neuronal and vascular mechanisms seem to play a role in the pathophysiology of FHM1, CADASIL and RVCL-S. The interaction between these mechanisms seems to be complex however, as increased CSD susceptibility did not associate well with an increased infarct volume and *vice versa*.

INTRODUCTION

Although migraine and stroke are distinct diseases, there is increasing evidence for comorbidity and overlapping pathology.^{1,2} Epidemiological studies have suggested that the link is more pronounced for migraine with aura,³ a migraine subtype in which the headache is preceded by transient focal neurological symptoms (“aura”).⁴ Human imaging and animal studies have indicated that cortical spreading depolarization (CSD), a wave of massive depolarization of neurons and glial cells that is accompanied by vasodilatation due to neurovascular coupling,¹ is the mechanism underlying the migraine aura.^{5,6} Waves with similar characteristics also occur in ischemic stroke, where they are referred to as peri-infarct depolarizations (PIDs).^{7,8} PIDs circle around the ischemic core, into the border zone (“penumbra”) thereby increasing the ischemic territory with each wave, due to, amongst others, paradoxical vasoconstriction and accompanying supply-demand mismatch.^{7,8} It has therefore been postulated that spreading depolarization (SD), with involvement of neuronal and vascular mechanisms, may explain the link between migraine and stroke.¹

The relation between migraine and stroke is also reflected in the clinical spectrum of various monogenic diseases.⁹ We envisaged that investigating transgenic mouse models for such disorders, and comparing measures of migraine (*i.e.* CSD) and stroke (*i.e.* ischemia after transient middle cerebral artery occlusion (MCAO)) in them, may shed light on the mechanisms relevant to migraine and stroke. Here we used mouse models for three disorders for which the relation between migraine and stroke (in patients and/or in animal studies) is most pronounced: Familial Hemiplegic Migraine type 1 (FHM1),¹⁰ Cerebral Autosomal Dominant Arteriopathy with Subcortical Infarcts and Leukoencephalopathy (CADASIL),¹¹ and Retinal Vasculopathy with Cerebral Leukoencephalopathy and Systemic manifestations (RVCL-S).¹² FHM1 is a monogenic form of migraine caused by specific missense mutations in CACNA1A that result in attacks of headache accompanied by an aura with hemiparesis.^{4,13} FHM1 exhibits a neuronal phenotype as shown by the enhanced neurotransmission and increased susceptibility to CSD in FHM1 mutant mice.¹⁴⁻¹⁶ FHM1 mice, either with the R192Q or the S218L mutation, were shown to also have an increased vulnerability to ischemic stroke, as evidenced by the increased infarct volume and decreased anoxic depolarization (AD) latency.¹⁷ Of note, a follow-up study only confirmed the infarct volume phenotype in the severer S218L mutant mice.¹⁸

CADASIL is a progressive small vessel disease caused by mutations involving cysteines in *NOTCH3* that result in ischemic strokes and (vascular) dementia.^{19,20} Notably, the presenting symptom of CADASIL in 40% of patients is migraine with aura.^{21,22} CADASIL exhibits a vascular phenotype as evidenced by an accumulation of mutant protein in vascular smooth muscle cells in a transgenic overexpressor mouse model for CADASIL.^{23,24} Of note, another CADASIL mouse model expressing a different NOTCH3 mutation also showed hallmarks of CADASIL, and interestingly, also an increased susceptibility for CSDs.²⁵

Finally, RVCL-S, which is caused by C-terminal truncating mutations in *TREX1* that cause systemic microvascular vasculopathy with white matter lesions.²⁶ Many patients with RVCL-S also have migraine.²⁶ RVCL-S exhibits a vascular (endothelial) phenotype but the exact mechanism that results in pathology is not known. An unpublished knock-in (KI) mouse model that expresses truncated Trex1 protein was generated and analyzed in the present study.

Given that disease onset in patients with CADASIL²⁷⁻²⁹ and with RVCL-S¹² typically occurs at middle age, but at relatively young age in patients with FHM,¹⁰ we compared readouts for migraine and ischemic stroke in young (3- to 6-month-old; both CSD and ischemic stroke) and old (12- to 14-month old; only ischemic stroke) FHM1, CADASIL and RVCL-S mice and the

appropriate wild-type (WT) control animals.

MATERIALS AND METHODS

Mice

Male homozygous transgenic mice of 3- to 6-month-old (both CSD and MCAO groups) and 12- to 14-month-old (only MCAO group) and appropriate WT control animals were used for the experiments. Mutant mice carried either the FHM1 missense mutation R192Q knock-in (KI)¹³ (strain R192Q), the CADASIL missense mutation R182Q³⁰ (overexpressor strain tgN3^{MUT350}) or the RVCL-S truncating mutation at residue 235³¹ (unpublished strain RVCL-S). For the FHM1 and RVCL-S strains non-transgenic littermates were used as controls (from this point on referred to as R192R and WT, respectively). Instead, for the CADASIL strain, mutant mice that carried a human genomic construct with the *NOTCH3* gene and the mutation were compared with transgenic mice that carried a similar construct but without the mutation strain tgN3^{WT}.²⁴ For the experiments, animals were randomized and researchers were blinded for genotype and age. Animals were housed in a controlled environment with food and water *ad libitum*. After the experiments genotypes were confirmed. All experiments were approved by the local committee for animal health, ethics and research of the Leiden University Medical Center.

Experimental Infarct Model

Ischemic stroke was induced using the MCAO model.³² During surgery, isoflurane (3% induction, 1.5% maintenance) in 70% pressurized air and 30% O₂ was used as anesthetic. Before surgery, pain relief medication was given (5 mg/kg, *s.c.*; Carporal, 50 mg/mL, AST Farma BV; Oudewater, the Netherlands). Body temperature of the mice was maintained at 37 ± 0.3°C during surgery using a feedback system including heating pad and rectal probe (FHC Inc.; Bowdoin, ME, USA). To occlude the MCA, a silicone-coated nylon monofilament (7017PK5Re; Docol Company, Redlands, CA, USA) was inserted via a small incision into the right common carotid artery. The origin of the MCA was blocked for 30 minutes, after which the filament was removed to allow for reperfusion. During surgery, cerebral blood flow (CBF) in the MCA territory was measured using Laser Doppler Flowmetry (PeriFlux System 5000; Perimed Järfälla-Stockholm, Sweden). Anoxic depolarization (AD) was measured using LDF and defined as the time between start of the MCA occlusion until the start of an additional subtle drop in blood flow, which is known to be the result of the first PID spreading through the brain tissue.³³ During a surgical recovery period of 2 hours, the mouse was allowed to wake up in a temperature-controlled incubator (V1200; Peco Services Ltd, Brough, UK). At the end of the experiment, *i.e.* after MRI and behavioral analyses (see below), mice were sacrificed using CO₂ and perfused transcardially with phosphate buffered saline and fresh 4% buffered PFA (Paraformaldehyde P6148; Sigma-Aldrich, St Louis, MO, USA) at 4°C and stored at -80 °C (for parallel histological studies).

MRI

At 4, 24 and 48 hours after MCAO surgery, mice were scanned (under isoflurane anesthesia; 3% induction, 1.5% maintenance in 70% pressurized air and 30% O₂) using a 7T small-animal MRI system (Bruker Pharmascan; Bruker, Ettlingen, Germany). A Multi Slice Multi Echo (MSME) sequence protocol was used with a TR/TE of 4.000 ms/ 9 ms, 20 echoes, 2 averages, matrix

128x128 mm, FOV of 2.50 cm, bandwidth 59523.8Hz, 16 slices with a thickness of 0.5 mm (no gap). Mice were allowed to wake up in a temperature-controlled incubator (Peco Services Ltd) for maximal 1 hour. Using Paravision 5.1 software (Bruker), quantitative T2-maps were calculated. Infarct volume was calculated using an automated lesion volume measurement tool.³⁴ In 5 MRI scans, large errors due to scan artifacts (as a result of movement or wrapping) were manually corrected.

Behavior analysis

Directly before surgery, directly before each MRI session, and 5 days after surgery, behavioral tests were performed and recorded. By analyzing the videos, the neurologic deficit score (NDS) was obtained using a 56-point neurological function scale.^{35,36} The score involved general and focal deficits, where 0 represents 'no deficits' and 56 represents 'poorest performance' in all categories. Categories concerning general appearance and performance include scores regarding fur (0–2), ears (0–2), eyes (0–4), posture (0–4), spontaneous activity (0–4), and epileptic behavior (0–12). Concerning focal deficits scores were stated for body asymmetry (0–4), gait (0–4), climbing on a 45° inclined surface (0–4), circling behavior (0–4), front-limb symmetry (0–4), compulsory circling (0–4), and whisker response to light touch (0–4).

Experimental cortical spreading depolarization

Separate groups of mice were anesthetized using 1.5% isoflurane in 20% O₂ and 80% N₂O. Blood gasses and mean arterial pressure values were monitored via a catheter in the left femoral artery, as described elsewhere.³⁷ In brief, after insertion of the catheter, an endotracheal tube was inserted in the trachea that allowed for artificial ventilation (MiniVent Ventilator, Model 845, Harvard Apparatus, Holliston, MA, USA). Arterial blood gasses (pCO₂, pO₂) and pH were measured at the start and end of the recordings and were maintained within normal limits (adjusting ventilation when needed). For CSD induction, the mouse was placed in a stereotactic frame (David Kopf Instruments, Tujunga, CA, USA). Core body temperature was maintained at 37°C ± 0.3°C. After exposure of the skull, three burr holes over the right hemisphere were prepared at the following coordinates: (I) for CSD induction on the occipital cortex (3.5 mm posterior, 2.0 mm lateral from bregma), (II) recording electrode in the frontal cortex (1.0 mm anterior, 2.0 mm lateral from bregma), and (III) recording electrode in the parietal cortex (1.0 mm posterior, 2.0 mm lateral from bregma). At the recording sites, a sharp glass capillary electrode (FHC Inc.) filled with 150 mM NaCl was advanced to a depth of 200–300 µm. DC-potential signals were measured with respect to an Ag/AgCl reference electrode placed subcutaneously in the neck of the animal. A reversible DC-deflection with an amplitude >5 mV was considered positive concerning a CSD event. Data were sampled (200 Hz), amplified (10X) and low-pass filtered at 4 Hz and analyzed off-line using LabChart software (ADInstruments, Colorado Springs, CO, USA). CSD events were induced by placement of a cotton ball soaked in 300 mM KCl on the dura for 30 minutes, with refreshment of the cotton ball every 15 minutes. The total number of CSD events that occurred within 30 minutes was used to calculate the frequency per hour. The time a first CSD event needed to travel from the first (parietal) measurement electrode to the second one (frontal) was used to calculate the propagation rate.

Statistics

Statistical analyses were performed in SPSS (SPSS Statistics 23, IBM Corporation, Armonk, NY,

USA). CSD frequency and propagation rate (mean \pm SEM) were analyzed between mutant and WT mice using a two-tailed Mann-Whitney U test. Time until occurrence of AD during MCAO (mean \pm SEM) for both ages was analyzed per genotype and accompanying WT using univariate ANOVA. Infarct volume and NDS were compared between mutant and WT mice using marginal mixed-models analyses. Data are shown as estimated marginal means \pm SEM. Survival analyses post-OK were performed using the Log-rank (Mantel-Cox) test. P-values <0.05 were considered to indicate statistical significance.

RESULTS

CSD frequency and propagation rate

Young FHM1 mutant mice showed an increased frequency (R192Q (n = 8): 18.3 ± 0.6 vs R192R (n = 7): 9.7 ± 0.7 , $p < 0.001$) and propagation rate (R192Q: 5.4 ± 0.7 vs R192R: 3.3 ± 0.5 , $p = 0.009$) of CSD (Figure 1A and B). For CADASIL mice of the same age group, no genotypic difference was observed for frequency (tgN3^{MUT350} (n = 2): 9.1 ± 3.2 vs tgN3^{WT} (n = 3): 9.9 ± 1.6) or propagation rate (tgN3^{MUT350}: 3.1 ± 0.5 vs tgN3^{WT}: 2.8 ± 0.1) of CSD, but the group sizes were too small to perform statistical analyses (Figure 1A and B). For RVCL-S mice no genotypic difference was observed for frequency (RVCL-S KI (n = 9): 9.1 ± 1.8 vs WT (n = 8): 9.9 ± 1.0) or

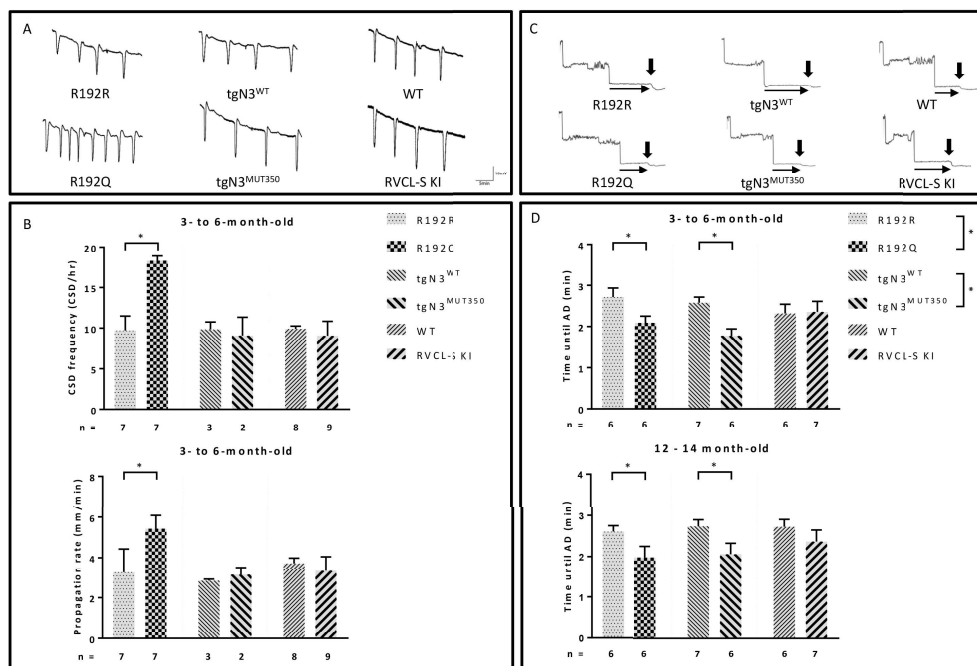


Figure 1. CSD and AD characteristics in FHM1, CADASIL and RVCL-S KI mice. (A) CSD example traces and (B) CSD frequency in WT and mutant FHM1 (R192Q), CADASIL (tgN3^{MUT350}) and RVCL-S KI mice (3- to 6-month-old). Only FHM1 mutant mice display enhanced CSD frequency and propagation rate. (mean \pm SEM, * $p < 0.05$). (C) Laser Doppler example traces of 3- to 6-month-old mice of the various genotypes show cerebral blood flow (CBF) reduction at the time of common carotid artery occlusion that is followed by a transient occlusion of the middle cerebral artery. The third decline in CBF shows the onset of anoxic depolarization (AD) and represents vasoconstriction of ischemic microvasculature due to tissue depolarization. (D) AD latency of 3- to 6-month-old and 12- to 14-month-old mice of the various genotypes show a decreased latency in FHM1 and CADASIL mutant mice, but not in the RVCL-S KI mutant mice. (mean \pm SEM, * $p < 0.05$). SEM = Standard Error of the Mean.

propagation rate (RVCL-S KI: 3.3 ± 0.7 : 3.7 ± 0.7) of CSD (Figure 1A and B).

Latency of anoxic depolarization

FHM1 mutant mice of both young and old age groups showed a decrease in AD latency ($F(1, 24) = 7.93$, $p = 0.010$; young mice: R192Q ($n = 6$): 2.2 ± 0.2 vs R192R ($n = 6$): 2.6 ± 0.3 ; and old mice: R192Q: 2.1 ± 0.4 ($n = 9$) vs R192R: 2.5 ± 0.2 ($n = 7$)) (Figure 1C and D). Also CADASIL mutant mice of both age groups had a decrease in AD latency ($F(1, 22) = 16.38$, $p = 0.001$; young mice: tgN3^{MUT350} ($n = 6$): 2.0 ± 0.2 ($n = 6$) vs tgN3^{WT} ($n = 7$): 2.5 ± 0.2 ; and old mice: tgN3^{MUT350} ($n = 6$) 2.1 ± 0.3 vs tgN3^{WT} ($n = 7$) 2.6 ± 0.2) (Figure 1C and D). However, no genotypic difference was found for AD latency in RVCL-S KI mutant mice (young mice: RVCL-S KI ($n = 7$): 2.3 ± 0.3 vs WT ($n = 6$): 2.3 ± 0.3 ; and old mice: RVCL-S KI ($n = 8$): 2.3 ± 0.5 vs WT ($n = 9$): 2.5 ± 0.3) (Figure 1C and D).

Infarct volume

With respect to infarct volume and evolution of infarct volume over time, no genotypic difference was found for FHM1 and CADASIL, for both young and old mice (see Figure 2). Instead, for RVCL-S KI mice there was an overall genotypic difference ($p = 0.005$) that was mainly driven by the group of older mice in which infarct volume in the mutants was increased at all three time points (4 hours, RVCL-S KI: 60.4 ± 5.3 ($n = 8$) vs WT: 39.8 ± 4.7 ($n = 10$), $p = 0.007$; 24 hours, RVCL-S KI: 82.6 ± 7.8 ($n = 6$) vs WT: 52.9 ± 6.4 ($n = 10$), $p = 0.009$; and 48 hours, RVCL-S KI: 110.7 ± 12.7 ($n = 5$) vs WT: 58.4 ± 10.0 ($n = 9$), $p = 0.004$) (Figure 2).

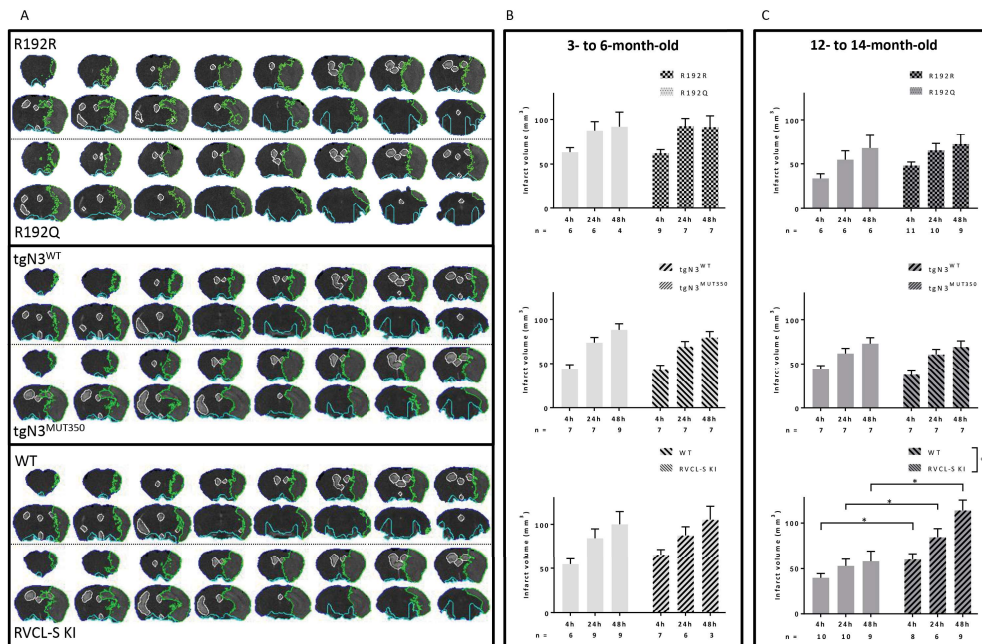


Figure 2. Infarct volume in FHM1, CADASIL and RVCL-S KI mice. (A) MRI example sections at 24 hours post MCAO in WT and mutant mice of the various genotype groups (3- to 6-month-old). (B) Stroke volumes at 4, 24 and 48 hours after MCAO in mutant and WT mice of 3- to 6-month-old and (C) 12- to 14-month-old (mean \pm SEM, $*p < 0.05$) reveal an overall increased infarct volume only for RVCL-S KI mutant mice, which was mainly driver by the infarct volumes of the older aged mice. SEM = Standard Error of the Mean.

Behavior analysis

Neither for the FHM1 nor the CADASIL mutant mice an overall genotypic difference (across both age groups) was found with respect to the neurologic deficit score (NDS) (Figure 3A). However, a sub-analysis showed that the NDS in mutant CADASIL mice was different for old mice at the two latest time points (24 hours, $\text{tgN3}^{\text{MUT350}}$: 23.0 ± 1.8 vs tgN3^{WT} : 16.0 ± 1.8 , $p = 0.01$; and 48 hours, $\text{tgN3}^{\text{MUT350}}$: 24.4 ± 2.1 vs tgN3^{WT} : 15.0 ± 2.2 , $p = 0.005$) (Figure 3B). An overall genotypic difference for (across both age groups) was observed for RVCL-S mice ($p = 0.005$). Sub-analysis showed that NDS was increased in old mice at all three time points (4 hours, RVCL-S KI: 31.4 ± 2.6 vs WT: 15.6 ± 2.4 , $p < 0.001$; 24 hours, RVCL-S KI: 26.4 ± 3.1 vs WT: 13.8 ± 2.7 , $p = 0.005$; and 48 hours, RVCL-S KI: 24.6 ± 3.3 vs WT: 13.1 ± 2.4 , $p = 0.012$) (Figure 3C).

Mortality rates were comparable between FHM and CADASIL mutant mice compared to the respective WT control groups for both age groups (Figure 4A and B). Instead, a trend was seen towards increased mortality for RVCL-S KI mice compared to WT control mice for both age groups (Figure 4C).

DISCUSSION

Here we compared characteristics of migraine (by induction of CSD) and ischemic stroke (by induction of an experimental infarct) in three monogenic models in which the relation between migraine and stroke is most prominent.

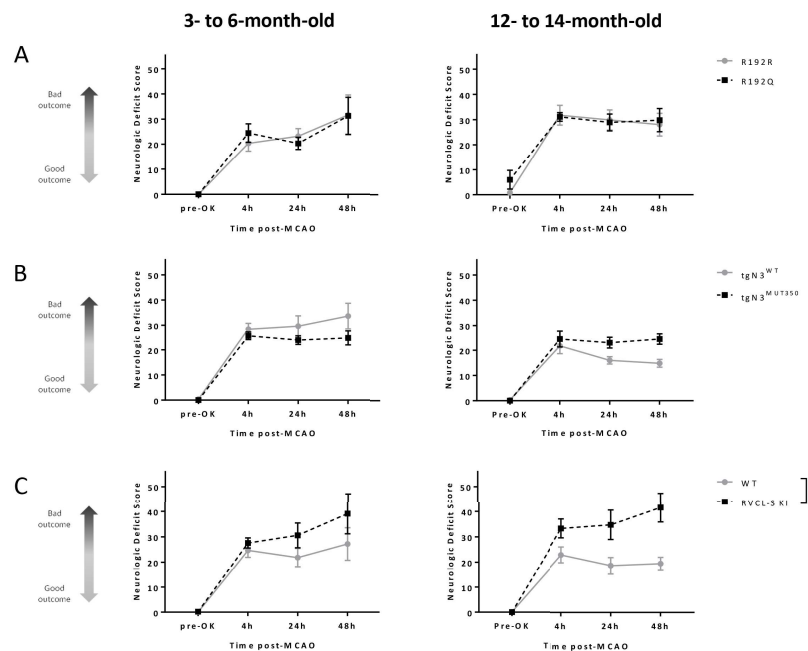


Figure 3. Behaviour analysis of FHM1, CADASIL and RVCL-S KI mice before and after ischemic stroke. Neurologic deficit scores pre-MCAO and at 4, 24 and 48 hours after surgery in the various mutant and WT mice of 3- to 6 and 12- to 14-month-old. (A) FHM1, (B) CADASIL and (C) RVCL-S KI. Figures reveal an overall worsened score only for RVCL-S mutant mice, which was mainly driver by the older aged mice (mean \pm SEM, * $p < 0.05$).

With respect to CSD susceptibility in (male) FHM1 mice, we observed an increased frequency and propagation rate as reported before (although in literature both readouts were not significantly different).³⁸ In fact, the absolute frequency was increased in our study compared to the previous study (~18 vs ~12/hour, respectively), whereas the absolute propagation rate was similar between studies (~5 vs ~4/min, respectively). In WT mice, frequency (~9 vs ~10/hour, respectively), and propagation rate (~2.5 vs ~3/min, respectively) were comparable between both studies. Moreover, whereas the observed decreased AD latency in the FHM1 R192Q mutants in response to MCAO was similar to what was described before (2.6 min vs 2.5 min, respectively),¹⁷ we did not observe the increased infarct volume in the mutant mice. Absolute values for infarct volume in WT mice in our study had a narrower range and were on average higher (~65 mm³ to ~85 mm³), compared to the data of the previous study¹⁷ (~35 mm³ to ~80 mm³).

This could, in hindsight, have led to the incorrect assumption that the infarct volume in the FHM1 mutant mice is increased compared to WT mice. An alternative, but less likely, explanation for the discrepancy between studies could be subtle differences in the MCAO surgery. Whereas we used the CCA as the entrance for the filament, in the previous described study the ECA was used. With both methods, the entrance artery stays occluded after surgery, which in our case could possibly have led to a higher infarct volume already in the WT animals that may have masked a small genotypic difference. Our rationale is supported by the fact that no increase in infarct size in FHM1 R192Q mice was found by the same researchers in a follow-up study.¹⁸ Moreover, the NDS and mortality rate also did not show a genotypic difference.

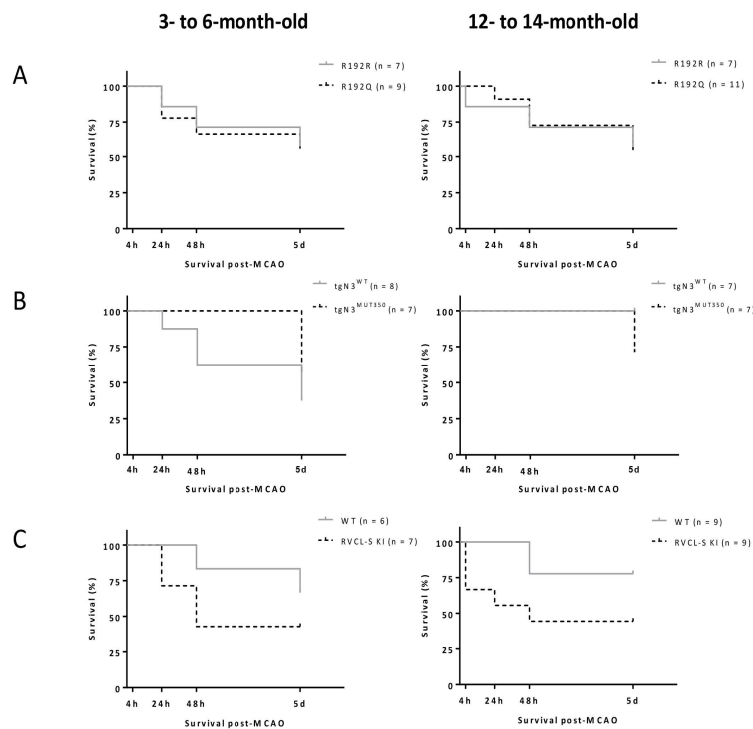


Figure 4. Mortality in FHM1, CADASIL and RVCL-S KI mice after induction of ischemic stroke. Mortality after MCAO surgery during the 5-day survival period for (A) FHM1, (B) CADASIL and (C) RVCL-S KI mutant mice and the respective control mice for both age groups.

With respect to CSD susceptibility in CADASIL mutant mice, we did not observe a genotypic difference for either frequency or propagation rate, unlike what has been reported.²⁵ Absolute values for the current and the previous study for frequency (WT: ~ 10 vs $\pm \sim 9$ /hour and mutant: ~ 9 vs ~ 11 /hour, respectively) and propagation (WT: ~ 2.5 vs ~ 2.5 /min and mutant: ~ 3.0 vs ~ 3.5 , respectively) were similar. This shows that the genotypic difference with respect to CSD characteristics is small and perhaps not relevant to explain disease pathophysiology; admittedly, by increasing the group sizes we may even find the previously observed genotypic difference. In this respect, it is important to point out that different types of CADASIL mutant lines were used in the two studies. Whereas Eikermann-Haerter *et al.*²⁵ used transgenic mice overexpressing human *NOTCH3* cDNA (driven by the SM22a smooth muscle cell promoter) containing CADASIL mutation Arg90Cys (TgNotch3^{R90C}),³⁹ we used transgenic mice in which human *NOTCH3* with the Arg182Cys mutation was overexpressed from a genomic human construct with endogenous regulatory elements present.²² Of note, expression of human mutant NOTCH in the tgN3^{MUT350} CADASIL line we used for our study was shown to be 350% of that of endogenous *NOTCH3* RNA expression,²⁴ whereas *NOTCH3* expression in the TgNotch3^{R90C} CADASIL line was <25% of endogenous expression.³⁹ This study is the first to investigate experimental stroke in CADASIL mutant mice. Given the vasculopathy seen in CADASIL patients and the, albeit, subtle difference in CSD characteristics reported earlier, we *a priori* expected a worsened stroke outcome in the mutant mice. Especially since we observed a decrease in AD latency in the young mutant mice, which would translate to a vasoconstrictive effect on the microvasculature.³³ Surprisingly, we did not find a genotypic difference in infarct volume, neither in young nor old mice. Given that CADASIL usually has a middle-aged onset, with infarct phenotype at an even later stage, it would be interesting to investigate even older (20- to 24-month-old) mice.

In the RVCL-S KI strain, we did not observe a genotypic difference for CSD frequency, propagation rate, nor AD latency, which is perhaps not surprising as these measures reflect mostly neuronal and partially vascular mechanisms³³ whereas RVCL-S is not a neuronal phenotype. Instead, we did observe an increased infarct volume and NDS, which could be the result of endothelial vascular dysfunction. Critical hypoperfusion that results in a lower ischemic threshold could lead to an increased infarct volume and perhaps also the subcortical brain lesions seen on MRI in RVCL-S patients.⁴⁰

We aimed to unravel molecular and neurobiological mechanisms of stroke and migraine concerning CSD and ischemic infarct characteristics. Both neuronal and vascular mechanisms, and the close interplay between them, are believed to play an important role in monogenic diseases as FHM1, CADASIL and RVCL-S. The relation appears complex because as illustrated by our finding that susceptibility to CSD does not directly correlate with infarct volume. Nevertheless, our finding support the notion that the relationship between migraine and stroke has both neuronal and vascular components.

REFERENCES

1. Dreier JP, Reiffurth C. The stroke-migraine depolarization continuum. *Neuron*. 2015;86:902-922
2. Hu X, Zhou Y, Zhao H, Peng C. Migraine and the risk of stroke: An updated meta-analysis of prospective cohort studies. *Neurol Sci*. 2017;38:33-40
3. Kurth T, Diener HC. Current views of the risk of stroke for migraine with and migraine without aura. *Curr Pain Headache Rep*. 2006;10:214-220
4. Headache Classification Committee of the International Headache S. The international classification of headache disorders, 3rd edition (beta version). *Cephalgia*. 2013;33:629-808
5. Hadjikhani N, Sanchez Del Rio M, Wu O, Schwartz D, Bakker D, Fischl B, et al. Mechanisms of migraine aura revealed by functional mri in human visual cortex. *Proc Natl Acad Sci USA*. 2001;98:4687-4692
6. Lauritzen M. Pathophysiology of the migraine aura. The spreading depression theory. *Brain*. 1994;117 (Pt 1):199-210
7. Dirnagl U, Iadecola C, Moskowitz MA. Pathobiology of ischaemic stroke: An integrated view. *Trends in Neurosciences*. 1999;22:391-397
8. Dreier JP, Major S, Manning A, Woitzik J, Drenckhahn C, Steinbrink J, et al. Cortical spreading ischaemia is a novel process involved in ischaemic damage in patients with aneurysmal subarachnoid haemorrhage. *Brain*. 2009;132:1866-1881
9. Ferrari MD, Klever RR, Terwindt GM, Ayata C, van den Maagdenberg AM. Migraine pathophysiology: Lessons from mouse models and human genetics. *Lancet Neurol*. 2015;14:65-80
10. de Vries B, Frants RR, Ferrari MD, van den Maagdenberg AM. Molecular genetics of migraine. *Hum Genet*. 2009;126:115-132
11. Dichgans M, Mayer M, Uttner I, Bruning R, Muller-Hocker J, Rungger G, et al. The phenotypic spectrum of cadasil: Clinical findings in 102 cases. *Ann Neurol*. 1998;44:731-739
12. Stam AH, Kothari PH, Shaikh A, Gschwendter A, Jen JC, Hodgkinson S, et al. Retinal vasculopathy with cerebral leukoencephalopathy and systemic manifestations. *Brain*. 2016; 139:2909-2922
13. Ophoff RA, Terwindt GM, Vergouwe MN, van Eijk R, Oefner PJ, Hoffman SM, et al. Familial hemiplegic migraine and episodic ataxia type-2 are caused by mutations in the ca2+ channel gene cacn1a4. *Cell*. 1996;87:543-552
14. Tottene A, Conti R, Fabbro A, Vecchia D, Shapovalova M, Santello M, et al. Enhanced excitatory transmission at cortical synapses as the basis for facilitated spreading depression in ca(v)2.1 knockin migraine mice. *Neuron*. 2009;61:762-773
15. van den Maagdenberg AM, Pietrobon D, Pizzorusso T, Kaja S, Broos LA, Cesetti T, et al. A cacna1a knockin migraine mouse model with increased susceptibility to cortical spreading depression. *Neuron*. 2004;41:701-710
16. van den Maagdenberg AM, Pizzorusso T, Kaja S, Terpolilli N, Shapovalova M, Hoebeek FE, et al. High cortical spreading depression susceptibility and migraine-associated symptoms in ca(v)2.1 s218l mice. *Ann Neurol*. 2010;67:85-98
17. Eikermann-Haerter K, Lee JH, Yuzawa I, Liu CH, Zhou Z, Shin HK, et al. Migraine mutations increase stroke vulnerability by facilitating ischemic depolarizations. *Circulation*. 2012;125:335-345
18. Eikermann-Haerter K, Lee JH, Yalcin N, Yu ES, Daneshmand A, Wei Y, et al. Migraine prophylaxis, ischemic depolarizations, and stroke outcomes in mice. *Stroke*. 2015;46:229-236
19. Amberla K, Waljas M, Tuominen S, Almkvist O, Poyhonen M, Tuisku S, et al. Insidious cognitive decline in cadasil. *Stroke*. 2004;35:1598-1602
20. Peters N, Opherck C, Danek A, Ballard C, Herzog J, Dichgans M. The pattern of cognitive performance in cadasil: A monogenic condition leading to subcortical ischemic vascular dementia. *Am J Psychiatry*. 2005;162:2078-2085
21. Guey S, Mawet J, Herve D, Duering M, Godin O, Jouvent E, et al. Prevalence and characteristics of migraine in cadasil. *Cephalgia*. 2015; 6:1038-1047
22. Tan RY, Markus HS. Cadasil: Migraine, encephalopathy, stroke and their inter-relationships. *PLoS One*. 2016;11:e0157613
23. Joutel A. Pathogenesis of cadasil: Transgenic and knock-out mice to probe function and dysfunction of the mutated gene, notch3, in the cerebrovasculature. *Bioessays*. 2011;33:73-80
24. Rutten JW, Klever RR, Hegeman IM, Poole DS, Dauwerse HG, Broos LA, et al. The notch3 score: A pre-clinical cadasil biomarker in a novel human genomic notch3 transgenic mouse model with early progressive vascular notch3 accumulation. *Acta Neuropathol Commun*. 2015;3:89
25. Eikermann-Haerter K, Yuzawa I, Dilekoz E, Joutel A, Moskowitz MA, Ayata C. Cerebral autosomal dominant arteriopathy with subcortical infarcts and leukoencephalopathy syndrome mutations increase susceptibility to spreading depression. *Ann Neurol*. 2011;69:413-418
26. Terwindt GM, Haan J, Ophoff RA, Groenen SM, Storimans CW, Lanser JB, et al. Clinical and genetic analysis of a large dutch family with autosomal dominant vascular retinopathy, migraine and raynaud's phenomenon. *Brain*. 1998;121 (Pt 2):303-316
27. Adib-Samii P, Brice G, Martin RJ, Markus HS. Clinical spectrum of cadasil and the effect of cardiovascular risk factors on phenotype: Study in 200 consecutively recruited individuals. *Stroke*. 2010;41:630-634
28. Desmond DW, Moroney JT, Lynch T, Chan S, Chin SS, Mohr JP. The natural history of cadasil: A pooled analysis of

previously published cases. *Stroke*. 1999;30:1230-1233

29. Opherk C, Peters N, Herzog J, Luedtke R, Dichgans M. Long-term prognosis and causes of death in cadasil: A retrospective study in 411 patients. *Brain*. 2004;127:2533-2539
30. Joutel A, Corpechot C, Ducros A, Vahedi K, Chabriat H, Mouton P, *et al.* Notch3 mutations in cadasil, a hereditary adult-onset condition causing stroke and dementia. *Nature*. 1996;383:707-710
31. Richards A, van den Maagdenberg AM, Jen JC, Kavanagh D, Bertram P, Spitzer D, *et al.* C-terminal truncations in human 3'-5' DNA exonuclease trex1 cause autosomal dominant retinal vasculopathy with cerebral leukodystrophy. *Nat Genet*. 2007;39:1068-1070
32. Longa EZ, Weinstein PR, Carlson S, Cummins R. Reversible middle cerebral artery occlusion without craniectomy in rats. *Stroke*. 1989;20:84-91
33. Shin HK, Dunn AK, Jones PB, Boas DA, Moskowitz MA, Ayata C. Vasoconstrictive neurovascular coupling during focal ischemic depolarizations. *J Cereb Blood Flow Metab*. 2006;26:1018-1030
34. Mulder IA, Khmelinskii A, Dzyubachyk O, de Jong S, Rieff N, Wermer MJ, *et al.* Automated ischemic lesion segmentation in mri mouse brain data after transient middle cerebral artery occlusion. *Front Neuroinform*. 2017;11:3
35. De Simoni MG, Storini C, Barba M, Catapano L, Arabia AM, Rossi E, *et al.* Neuroprotection by complement (c1) inhibitor in mouse transient brain ischemia. *J Cereb Blood Flow Metab*. 2003;23:232-239
36. Storini C, Rossi E, Marrella V, Distaso M, Veerhuis R, Vergani C, *et al.* C1-inhibitor protects against brain ischemia-reperfusion injury via inhibition of cell recruitment and inflammation. *Neurobiol Dis*. 2005;19:10-17
37. Shyti R, Eikermann-Haerter K, van Heiningen SH, Meijer OC, Ayata C, Joels M, *et al.* Stress hormone corticosterone enhances susceptibility to cortical spreading depression in familial hemiplegic migraine type 1 mutant mice. *Exp Neurol*. 2015;263:214-220
38. Eikermann-Haerter K, Dilekoz E, Kudo C, Savitz SI, Waeber C, Baum MJ, *et al.* Genetic and hormonal factors modulate spreading depression and transient hemiparesis in mouse models of familial hemiplegic migraine type 1. *J Clin Invest*. 2009;119:99-109
39. Ruchoux MM, Domenga V, Brulin P, Maciazek J, Limol S, Tournier-Lasserre E, *et al.* Transgenic mice expressing mutant notch3 develop vascular alterations characteristic of cerebral autosomal dominant arteriopathy with subcortical infarcts and leukoencephalopathy. *Am J Pathol*. 2003;162:329-342
40. Stam AH, Haan J, van den Maagdenberg AM, Ferrari MD, Terwindt GM. Migraine and genetic and acquired vasculopathies. *Cephalalgia*. 2009;29:1006-1017